

EDITOR COMMUNICATED PAPER

Co-infection of respiratory bacterium with severe acute respiratory syndrome coronavirus induces an exacerbated pneumonia in mice

Yasushi Ami, Noriyo Nagata, Kazuya Shirato, Rie Watanabe, Naoko Iwata, Keiko Nakagaki, Shuetsu Fukushi, Masayuki Saijo, Shigeru Morikawa and Fumihiro Taguchi

National Institute of Infectious Diseases, Murayama Branch, 4-7-1 Gakuen, Musashi-Murayama, Tokyo 208-0011, Japan

Correspondence

Fumihiro Taguchi, Department of Virology III, Division of Respiratory Virus Diseases, National Institute of Infectious Diseases, 4-7-1 Gakuen, Musashi-Murayama, Tokyo 208-0011, Japan.
Tel: +81-42-561-0771 (ext. 533);
email: ftaguchi@nih.go.jp

Received: 4 December 2007; accepted:
6 December 2007

List of Abbreviations: ACE2, angiotensin-converting enzyme 2; ARDS, acute respiratory distress syndrome; BAL, bronchoalveolar lavage; BSL 3, biosafety level three; DMEM, Dulbecco's modified minimal essential medium; FCS, fetal calf serum; FGF, fibroblast growth factor; Fr-1, Frankfurt-1; Fr-mo, Fr-1 passaged 10 times through mice; GM-CSF, granulocyte-macrophage colony stimulating factor; IFN, interferon; IL, interleukin; i.n., intranasally; IP, IFN-inducible protein; KC, keratinocyte-derived cytokine; LPS, lipopolysaccharide; MCP, monocyte-chemotactic protein; MHV, murine coronavirus mouse hepatitis virus; MIG, monokine-induced by IFN- γ ; PBS, phosphate buffered saline; p.i., post infection; *Pp*, *Pasteurella pneumotropica*; SARS, severe acute respiratory syndrome; SARS-CoV, severe acute respiratory syndrome coronavirus; TNF, tumor-necrosis factor; VEGF, vascular endothelial growth factor.

Key words

coronavirus, elastase, mouse, SARS.

ABSTRACT

SARS-CoV grows in a variety of tissues that express its receptor, although the mechanism for high replication in the lungs and severe respiratory illness is not well understood. We recently showed that elastase enhances SARS-CoV infection in cultured cells, which suggests that SARS development may be due to elastase-mediated, enhanced SARS-CoV infection in the lungs. To explore this possibility, we examined whether co-infection of mice with SARS-CoV and *Pp*, a low-pathogenic bacterium which elicits elastase production in the lungs, induces exacerbation of pneumonia. Mice co-infected with SARS-CoV and *Pp* developed severe respiratory disease with extensive weight loss, resulting in a 33~90% mortality rate. Mice with exacerbated pneumonia showed enhanced virus infection in the lungs and histopathological lesions similar to those found in human SARS cases. Intranasal administration of LPS, another elastase inducer, showed an effect similar to that of *Pp* infection. Thus, this study shows that exacerbated pneumonia in mice results from co-infection with SARS-CoV and a respiratory bacterium that induces elastase production in the lungs, suggesting a possible role for elastase in the exacerbation of pneumonia.

SARS-CoV is responsible for a life-threatening disease that affected nearly 800 individuals in 2002–2003 (1–3). The virus genome sequence of about 30 kilobases

was identified within the month after its isolation (4, 5). Its receptor, ACE2, was also discovered within several months of identification of the causative agent (6). The

advancement of SARS-CoV research has been overwhelming. This virus has become one of the most studied among the coronaviruses. In spite of these extensive studies, the pathogenesis and mechanisms of development of this severe respiratory disease have not yet been fully elucidated.

Although a number of animal species have been found to permit SARS-CoV replication (7–12), there has been only limited success in developing histopathology similar to that of human SARS in animal models. Recently, transgenic mice expressing human ACE2 were reported to develop pneumonia after SARS-CoV infection. The pathogenesis of SARS-CoV infection in those mice was, however, slightly different from that of human SARS (13, 14). Human SARS patients generally die from pulmonary failure, whereas infection of the central nervous system is the major factor responsible for a fatal outcome in transgenic mice (13). In another transgenic model, high replication of SARS-CoV in the brain likely contributed to the deaths (14). More recently, Roberts *et al.* (15) reported that a mouse-adapted SARS-CoV causes fatal respiratory disease in young mice, which reproduced many aspects of human SARS.

Respiratory agents, such as human metapneumovirus or chlamydia, have been isolated from SARS patients (1, 16), and were initially suspected to be the causative agents of SARS. However, SARS-CoV was finally identified as the agent of SARS, since it fulfilled Koch's postulate (7). Nevertheless, when animals were infected with SARS-CoV alone, most failed to develop SARS-like severe pneumonia (12). These results may imply that the respiratory agents found in some SARS cases could work in combination with SARS-CoV in order to induce a severe form of pneumonia.

In the course of studying the cell entry mechanism for SARS-CoV, we found that some proteases produced in the host animals, such as trypsin and elastase, enhanced SARS-CoV infection in cultured cells (17). These *in vitro* observations hinted at the highly pathogenic feature of this virus in the lungs, where elastase is predominantly produced as a result of inflammation. In the present study, we examined whether or not SARS-CoV infection is enhanced by weak inflammation in the lungs induced by infection with low-pathogenic bacteria which induce elastase. Our results show that both low-virulent *Pp* infection, and administration of LPS derived from *Escherichia coli*, induced elastase in the lungs and enhanced the replication of SARS-CoV, resulting in exacerbation of the respiratory disease caused by SARS-CoV infection and a high mortality rate. These results indicate that co-infection of SARS-CoV with low-virulent microorganisms induces exacerbated pneumonia and suggest the possibility that elastase is involved in the pathogenesis of exacerbated pneumonia caused by SARS-CoV infection.

MATERIALS AND METHODS

Virus and virus titration

Fr-1 (1, 18) kindly provided by Dr. John Ziebuhr, as well as Fr-mo, was propagated and plaque assayed with VeroE6 cells as previously described (17). Compared with the original virus, Fr-1 used in our laboratory has two amino acid changes, at position 641 (His to Tyr) of S protein and ORF1a 429 (Ala to Ser) (18), which are presumed to have arisen during passage through VeroE6 cells.

Passage of Fr-1 through mice to obtain Fr-mo was done as follows. Mice were inoculated *i.n.* with 20 μ l of Fr-1 and their lungs were washed with PBS (pH 7.2), containing 0.1% bovine serum albumin (Sigma, St Louis, MO, USA), 20 IU of penicillin G (Sigma), 20 μ l of streptomycin (Sigma) and 1 μ g of amphotericin B (Gibco, Grand Island, NY, USA) per ml on day three after infection. The resultant bronchoalveolar wash was inoculated into mice by the *i.n.* route and passaged a total of 10 times. Finally, the lungs of the infected mice were homogenized and the homogenate was spun at 2000 rpm for 10 minutes at 4°C. The supernatant was inoculated onto VeroE6 cells, and culture fluid from infected cells was used to infect the mice. Fr-mo has amino-acid mutations in the S protein at positions 480 (Asp to Glu) as well as 641 (His to Tyr); the latter is identical to the mutation found in Fr-1. Fr-mo has two additional mutations in the ORF1a 3534 (Phe to Leu) and ORF1ab 5172 (Thr to Ile), though the mutation at ORF1a 429 found in Fr-1 was not present.

For titration of virus, the lungs were aseptically isolated at intervals after inoculation and 10% homogenates were prepared by using a grinder and silica sand in chilled PBS containing 200 μ g/ml of kanamycin (Meiji-seika, Tokyo, Japan). The homogenates were centrifuged at 2000 rpm for 10 minutes at 4°C. The supernatants were isolated and kept at -80°C until virus titration. VeroE6 cells were grown and maintained in DMEM (Nissui, Tokyo, Japan) containing 5% FCS (Sigma) and virus infectivity was determined by plaque assay as described previously (17).

Mice

Six-week-old BALB/c male mice were purchased from SLC (Hamamatsu, Japan) or Charles River Japan (CRJ, Tokyo, Japan). Those mice are serologically confirmed to be free from infections with pathogenic microorganisms including *Pp*. Mice were anesthetized with intraperitoneal administration of xylazine and ketamine and inoculated *i.n.* with 20 μ l of *Pp* MaM strain (19) suspended in PBS. In some experiments, mice were administered *i.n.* with 20 μ l of LPS O55:B5 (Sigma) dissolved in PBS at a concentration of 1 mg/ml. Those mice were inoculated *i.n.* with 20 μ l of

SRAS-CoV one day after *Pp* infection or LPS administration and kept in globe box isolators in a BSL 3 laboratory in our institute during the experimental period. Mice were killed at selected intervals after SARS-CoV infection, and lungs and other organs were aseptically collected for virus titration, histopathological examination, detection of virus-specific antigens and measurement of elastase activity. Mice were maintained in keeping with the animal experiment guidelines of our institute.

Histopathology and immunohistochemistry

Mice inoculated with *Pp* and/or SARS-CoV were killed at selected intervals after infection. Tissues from those mice were fixed in 10% neutral buffered formalin (pH 7.4) and subjected to routine pathological examination. For detection of virus antigens, streptavidin-biotin complex methods (DAKO, Japan) were used with rabbit hyperimmune serum produced in our institute against SARS-CoV according to the manufacturer's instructions.

Elastase activity

Elastase activity was examined using the synthetic substrate Suc-Ala-Ala-Pro-Val-pNA, which is highly specific for neutrophil elastase in lung tissue, as described by Yoshimura *et al.* (20). To determine elastase activity, we employed 10% lung homogenates, prepared as described above, or BAL. For the collection of BAL, one ml of chilled saline containing 0.38% citric acid was injected into the lungs of dead mice via the trachea using a canula combined with a syringe and then the saline was recovered. After removing cells containing in the BAL by spinning at 10000 rpm for five minutes, supernatants were used to determine elastase activity. The lung homogenates diluted 10-fold with PBS (finally 1% lung homogenates) or BAL were incubated in 0.1 M Tris-HCl buffer (pH 8.0) containing 0.5 M NaCl and 1 mM substrate for 24 hours at 37°C. pNA released from the substrate was measured spectrophotometrically at 405 nm and shown as elastase activity as described previously (20).

Analysis of cytokines and chemokines

Cytokines and chemokines were assayed mostly as previously reported (9). Lung homogenates prepared as described above were diluted 10 times with a lysis buffer. Viruses included in the materials were completely inactivated by ultraviolet irradiation for 10 minutes. Using a Mouse cytokine 20 plex antibody bead kit (Bioscience International, Inc., Camarillo, CA, USA) as previously reported (9), these materials were examined with Luminex 200 (Luminex Co, Austin, TX, USA) for the following cytokines and chemokines, FGF basic, GM-CSF, IFN- γ ,

IL-10, IL-12, IL-13, IL-17, IL-1 α , IL-1 β , IL-2, IL-4, IL-5, IL-6, IL-10, KC, MCP-1, MIG, IP-10, TNF- α , VEGF.

RESULTS

Induction of elastase in mouse lungs by *Pp* infection and its effect on respiratory disease caused by SARS-CoV infection

It has been shown that SARS-CoV replication is enhanced in the presence of proteases such as trypsin or elastase (17). The possible molecular mechanism of this enhancement is the potentiation of SARS-CoV infection from the cell surface, which is more efficient than the infection via an endosomal pathway which takes place in the absence of proteases (17). Elastase, a major protease produced in lung inflammation, could enhance SARS-CoV replication in the lungs, which would, in turn, result in severe damage to this organ. We first examined whether infection with *Pp* induced elastase in the lungs. *Pp* is of low virulence and, as a rule, causes only mild, never severe, respiratory disease in adult mice (21). Six-week-old BALB/c mice were infected i.n. with 2.0×10^7 c.f.u. of *Pp*, and elastase activity in both lung homogenates and BAL was monitored. At one day p.i., significant amounts of elastase were detected in the BAL and lungs of *Pp*-infected mice, while elastase activity was undetectable in samples from uninfected mice (Fig. 1a). We also examined the effect of LPS administration on elastase production in the lungs, since LPS has been used as an elastase inducer (22). Mice administered i.n. with 20 μ l of LPS (1 mg/ml) dissolved in PBS were shown to produce elastase in the lungs one to two days after administration, similar to infection with *Pp* (Fig. 1b). These results show that *Pp* and LPS are appropriate agents for inducing elastase in the lungs and BAL.

Next, we examined the effect of *Pp* on SARS-CoV infection. We used two different SARS-CoVs; one was Fr-1 isolated from diseased humans (1, 18) and the other a mouse-adapted virus called Fr-mo which was passaged 10 times through the mice and finally grown in VeroE6 cells as described in Materials and Methods. Fr-mo has four amino acid changes in the spike, ORF1a and ORF1b compared with those of Fr-1 reported previously (18). Mice were infected with 1.3×10^7 c.f.u. of *Pp* and, one day later, were co-infected with 1.1×10^6 and 0.8×10^6 p.f.u. of Fr-1 and Fr-mo, respectively, by the i.n. route. As shown in Figures 2a and b, mice inoculated with *Pp* alone showed a transient loss of body weight and ruffled hair from one to four days pi. Mice infected with Fr-1 or Fr-mo alone rarely showed weight loss and ruffled hair. When mice were infected with both *Pp* and Fr-1, the clinical symptoms were similar to those of mice inoculated with *Pp* alone, and included transient loss of body weight and ruffled hair

Fig. 1. Elastase production in the lungs of mice after *Pp* infection or LPS administration. Mice inoculated i.n. with 1.5×10^7 cfu of *Pp* suspended in $20 \mu\text{l}$ PBS (+) or mock-infected mice (-) were killed one day after infection and elastase activity in BAL and lung homogenates were measured (a). Mice were inoculated i.n. with 2.3×10^7 cfu of *Pp* or administered with $20 \mu\text{l}$ of LPS (1 mg/ml) dissolved in PBS and elastase activity in lung homogenates was determined one and two days after inoculation. Mock-infected mice (No) were also examined for elastase activity (b). Mean values with standard deviation of three to five samples in each group are shown.

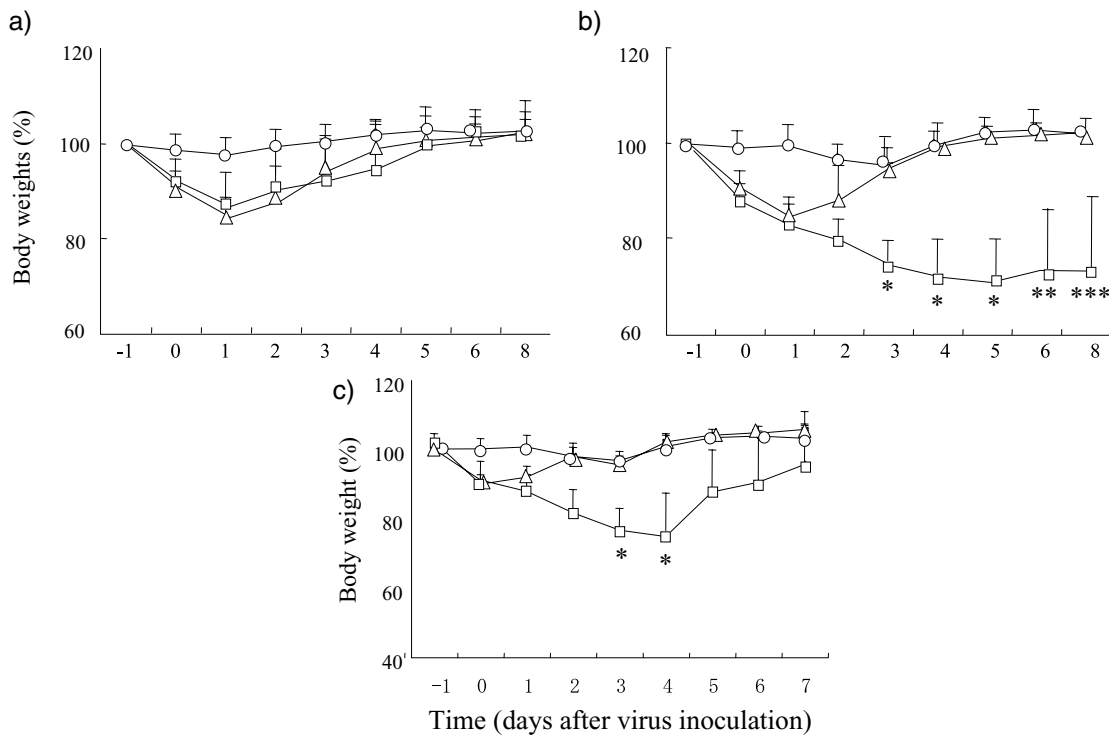
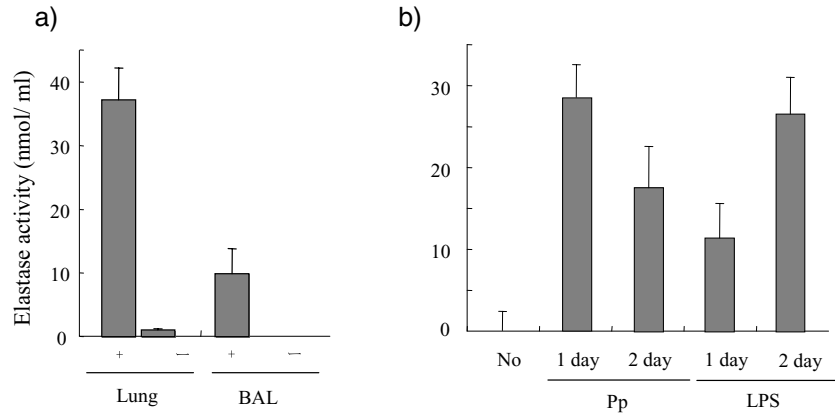


Fig. 2. Body weights of mice infected with SARS-CoV. Mice were infected i.n. with *Pp* (1.3×10^7 cfu) and 1 day later with SARS-CoV, either 1.1×10^6 of p.f.u. Fr-1 (a) or 0.8×10^6 p.f.u. of Fr-mo (b), and were weighed daily after *Pp* infection. Mice were administered i.n. with $20 \mu\text{l}$ of LPS (1 mg/ml), infected with 0.8×10^6 p.f.u. of Fr-mo 1 day later and weighed daily after LPS administration (c). Mean body weights are shown as a percentage compared with the mean weights of all mice measured just before *Pp* or LPS inoculation. Mice were inoculated with

SARS-CoV alone (○), *Pp* or LPS alone (△) or *Pp* or LPS + SARS-CoV (□). Two of six mice infected with *Pp* + Fr-mo died by day five p.i., and the body weight from days five to seven p.i. showed a significant difference when compared with those of *Pp*-infected mice (* $P < 0.001$, ** $P < 0.005$, *** $P < 0.01$ by Student's t test) (b). Three of six mice treated with LPS and infected with Fr-mo died on day four, and body weights were significantly lower (* $P < 0.001$) on days three to four in comparison to those of mice treated with LPS alone (c).

(Fig. 2a). In contrast, mice co-infected with *Pp* + Fr-mo had severe weight loss, and most of them did not recover during the observation period (eight days p.i.) (Fig. 2b). Those mice showed clinical symptoms, such as ruffled

hair from one day after *Pp* infection and hunched posture from three to four days after Fr-mo infection. These symptoms continued during the observation period. On days four to eight p.i., these mice lost 30% or greater

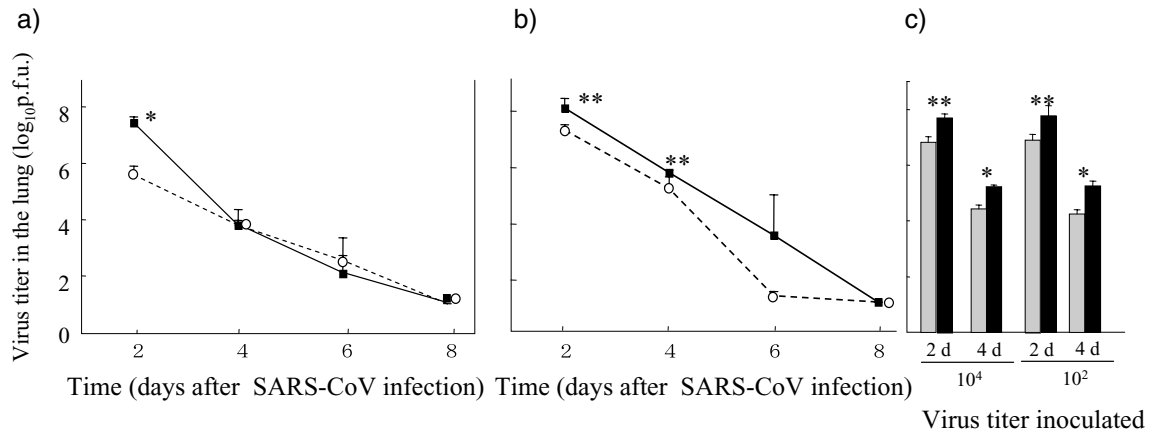


Fig. 3. Virus titers in the lungs of mice infected with *Pp* and/ or SARS-CoV: Mice infected (solid line) or mock-infected (broken line) with *Pp* and one day later with Fr-1 (a) or Fr-mo (b), as described in the legend to Fig. 2, were killed on days two, four, six and eight, and virus titers in the lungs were determined by a plaque assay. Significant difference was shown (* $P < 0.001$, ** $P < 0.01$ by Student's *t* test) (a and b). Mice were infected with *Pp* (2.0×10^7 cfu) (black column) or mock-infected

(shaded column) and one day later further infected with 1×10^4 (10^4) or 1×10^2 (10^2) p.f.u. of Fr-mo. Virus titers in the lungs were examined on days two (2 d) and four (4 d) after Fr-mo infection (c). Significant difference was shown (* $P < 0.001$, ** $P < 0.006$ by Student's *t* test) (c). Virus titers are indicated in p.f.u. in $\log_{10}/50$ mg tissue weight. Mean values of the titers with standard deviation are shown. Groups a and b consisted of four to five mice each and group c three mice.

of their body weight, and more than 33% of those mice died after exhibiting severe respiratory disease. Thus, mice co-infected with *Pp* + Fr-mo developed severe respiratory disease, suggesting the possibility that elastase produced by *Pp* infection exacerbated infection by SARS-CoV adapted to mice. We also infected mice that had been administered LPS with Fr-mo (Fig. 2c). These mice developed weight loss and clinical symptoms similar to those displayed by mice inoculated with *Pp* + Fr-mo. One-half of the infected mice died by day four p.i., but the remaining mice gradually recovered (Fig. 2c). This finding also supported the possibility that elastase is involved in the exacerbation of respiratory disease caused by SARS-CoV infection.

Effect of *Pp* infection on virus growth in the lungs

We then examined the virus titers of mice infected with SARS-CoV alone and those doubly infected with *Pp* and SARS-CoV. Those mice were infected under conditions identical to those shown in Figure 2. When examined on days two and four p.i., Fr-mo had grown at a rate 10- to 50-fold higher in the lungs of mice than had Fr-1, (Fig. 3a and b), showing that Fr-mo has a higher potential to grow in mice. On day two p.i. virus titers in the lungs were about 100-fold higher in mice infected with *Pp* and Fr-1 than in mice infected with Fr-1 alone. However, by the fourth day p.i., there was not a significant difference between the two groups (Fig. 3a). On day two p.i. the virus

titers of mice infected with *Pp* + Fr-mo were slightly, but significantly higher than those of mice infected with Fr-mo alone. The difference in virus titers between mice infected with *Pp* + Fr-mo and those with Fr-mo alone was also evident at four days p.i. (Fig. 3b). These results show that infection with *Pp* greatly enhanced the infection of Fr-1, but had a less remarkable effect in the infection of Fr-mo in the early phase of viral infection. More significant enhancement of Fr-mo infection was observed when mice were infected with low titers of virus. When mice were infected with 1×10^4 or 1×10^2 p.f.u., the virus titers were about 10-fold higher in mice co-infected with *Pp* + Fr-mo than in those infected with Fr-mo alone on both two and four days p.i. (Fig. 3c). Enhancement of Fr-mo infection in the lungs was also observed in mice that had received LPS as compared with mice without LPS administration (data not shown). These results collectively suggest that the elastase induced by *Pp* infection or LPS administration enhanced the infection produced by mouse-adapted Fr-mo in mouse lungs.

The elastase activities of those mice infected with Fr-1, *Pp* and Fr-1, Fr-mo, *Pp* + Fr-mo or *Pp* alone were examined on days two and four after SARS-CoV infection, that is, three and five days after *Pp* infection. As shown in Figure 4, the lung elastase activity of mice infected with *Pp* was significantly higher than that in mice not infected with *Pp*, when they were examined on day two, but not on day four, after SARS-CoV infection. It was also clear that neither Fr-1 nor Fr-mo elicited elastase by themselves. These

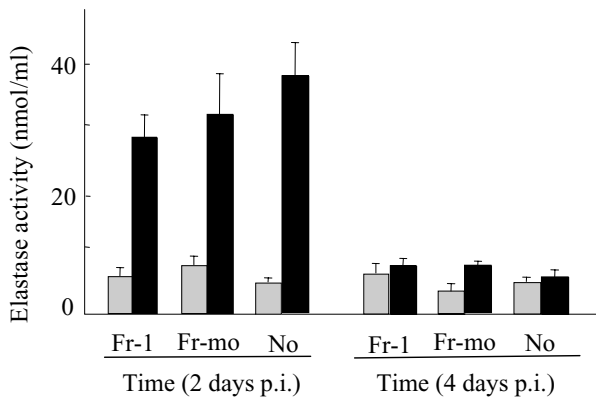


Fig. 4. Elastase activity in the lung of mice infected with *Pp* and SARS-CoV. Lung homogenates from mice infected with *Pp* (black column) or mock- infected mice (shaded column) prepared on day two and four after SARS-CoV (Fr-1, Fr-mo) or mock (no) infection were examined for elastase activity. Mean values of elastase activity with standard deviation are shown.

data, together with the findings from virus titers in the lungs shown in Figures 3a and b, indicate the possibility that elastase produced in the lungs following *Pp* infection efficiently (about 100-fold) enhanced Fr-1 infection, and not so efficiently (less than 10-fold), but still significantly enhanced, Fr-mo infection. However, the slightly higher titers found four days p.i. in the lungs of mice infected with *Pp* + Fr-mo could not be explained by the direct influence of elastase on Fr-mo infection in the lungs. An important condition for sustaining high titers beyond four days p.i. would be that of high replication in the lungs in an early phase of infection, which could be facilitated by elastase induced by *Pp*. These data suggest that severe respiratory disease caused by co-infection of *Pp* and mouse-adapted SARS-CoV is attributable to the high replication of virus in the lungs, for which the elastase produced by *Pp* infection is probably responsible.

Development of severe pneumonia in infected mice was not due to high growth of *Pp* in the lungs, since almost no bacteria were detected in mice co-infected with *Pp* and SARS-CoV on day four of *Pp* infection. This was similar to the findings after infection with *Pp* alone. We have also examined infectious virus titers in various organs other than the lungs. The blood, liver, spleen, heart, intestines and brain from mice doubly infected with *Pp* + Fr-mo, contained infectious viruses not significantly higher than 10^3 p.f.u./50 mg tissues, indicating that Fr-mo failed to grow in organs other than the lungs.

Since involvement of cytokines on the pathogenesis of SARS has been described (9, 13–15), we measured the levels of a number of cytokines in the lungs of mice infected with Fr-mo alone that failed to develop severe pneumonia, and in the lungs of those co-infected with *Pp* + Fr-mo

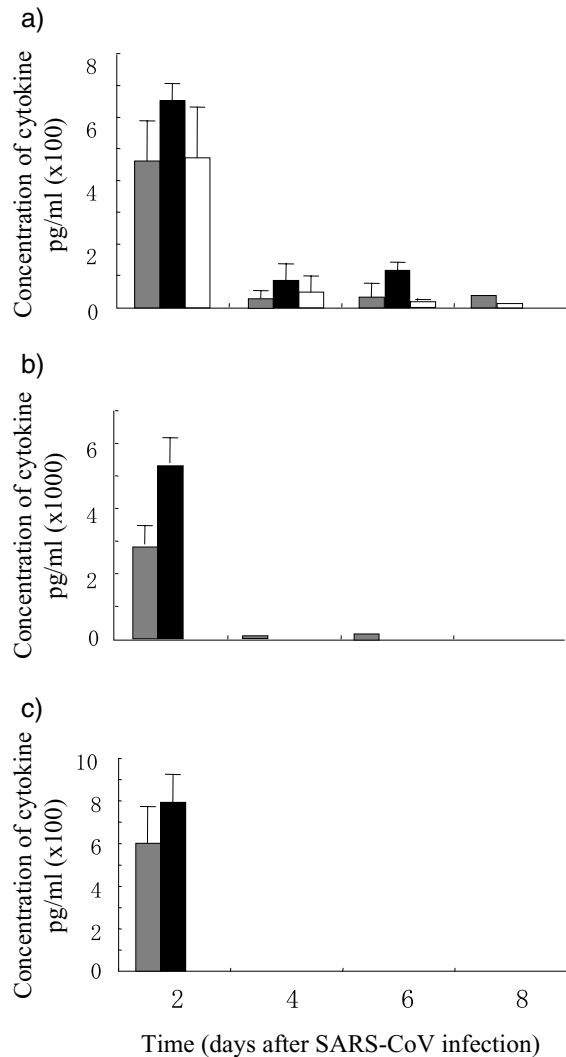


Fig. 5. Comparison of cytokine concentrations in mice infected with *Pp* alone, Fr-mo alone and those infected with *Pp* + Fr-mo. Lung homogenates from Fr-mo infected mice (shaded column) and *Pp* + Fr-mo infected mice (black column) were examined for 20 different cytokines. Lung homogenates prepared from mice infected with *Pp* alone (white column) were also examined. The concentrations of three cytokines, IL-1 α (a), IP-10 (b) and MIG (c) are illustrated, of which IP-10 and MIG were significantly higher in the *Pp* + Fr-mo infected mice than those infected with Fr-mo alone, by Student's t test (IP-10: $P < 0.0025$, MIG: $P < 0.015$, IL-1 α : $P = 0.061$).

showing exacerbated pneumonia. As shown in Figure 5, significantly higher levels of production of two cytokines, IP-10 (Fig. 5b) and MIG (Fig. 5c), were encountered in the latter mice on day two p.i., but not later than day four. IL-1 α (Fig. 5a) was also significantly higher in *Pp* + Fr-mo infected mice ($P = 0.024$), however, there was no significant difference between *Pp* infected mice and those infected with *Pp* + Fr-mo ($P = 0.061$). The levels of the other

17 cytokines were not significantly different between those infected with Fr-mo and doubly infected mice. These results could suggest the involvement of those two cytokines in the high pathogenesis caused by co-infection with *Pp* and SARS-CoV.

Histopathology of exacerbated pneumonia

We have examined histopathological changes in the lungs of mice in which virus titers were measured as shown in Figure 3. Mice infected with *Pp* alone showed consolidation with neutrophils and macrophage accumulation, but these lesions were cured after a week or so. Mice infected with SARS-CoV alone had an infiltration of inflammatory mononuclear cells in the alveolar walls. Co-infected mice displayed both of those lesions at an early phase of infection. On day four *p.i.*, *Pp* + Fr-mo-infected mice showed a plentitude of eosinophilic hyaline substances in cavities filled with necrotic cell debris and alveolar macrophages as well as hyperplastic changes of type 2 respiratory epithelium (Fig. 6a), although these changes in the alveoli were hardly observed in mice infected with Fr-mo alone (Fig. 6b). Viral antigens were detected in the cytoplasm of type 1 and 2 respiratory epithelial cells, as well as in exfoliative broncho-epithelial cells in alveolar cavities (Fig. 6c). Co-infected mice that died on days four to six displayed diffuse alveolar damage, such as severe congestion, diffuse exudation of hyaline substance into alveolar cavities, low inflammatory cell infiltration and type 2 respiratory epithelial cell activation (Fig. 6d, e), all of which was reminiscent of that seen in cases of ARDS reported following autopsy of victims of the latest SARS epidemic (23, 24). Thus, great histopathological similarities were found to exist between mice infected with *Pp* + Fr-mo and the SARS cases reported in 2003.

DISCUSSION

There are several reports that mice are susceptible to SARS-CoV infection (11, 25, 26). They also show that the diseases caused by this viral infection were asymptomatic, and that only transient replication of virus took place in the lungs of the mice. Also, with a few exceptions, many other species of animals shown to be susceptible to SARS-CoV infection did not develop an exacerbated respiratory disease (27–29). The present study showed that we could induce a severe respiratory disease in mice resembling that found in humans with SARS-CoV infection. Mice co-infected with low-virulent respiratory bacterium *Pp* and SARS-CoV developed severe pneumonia and more than 35% of infected mice died. The present study indicates that two conditions are critical for the establishment of severe disease, both of which were documented to be important for development

of SARS. One is the enhancement of SARS-CoV infection by proteases produced by the host cells (17). The other is the evolution of SARS-CoV to an extent that it can become highly infectious and pathogenic to a given species of animals to which SARS-CoV is adapted (15, 19, 30, 31). When these two conditions are fulfilled, severe respiratory disease can be reproduced.

Roberts *et al.* described that SARS-CoV adapted to mice by serial passage of the original Urbani strain in mouse lungs acquired high virulence for mice (15). The mouse-adapted virus has several genetic mutations accompanying the amino acid mutations not only in the S but also M, ORF1a and 1b genes. Recombinant viruses containing mutations in the S and M alone or those containing mutations in ORF1a and 1b alone were not highly virulent, but viruses with mutations in all of those genes showed a high virulence, indicating that the virulence of SARS-CoV is determined by multiple genes. Similar observations were reported from Weiss's laboratory for MHV infection. They reported that S is a major determinant of the neurovirulence of MHV-JHM strain, but that genes outside the S are also involved in virulence (31, 32). Mouse-adapted Fr-mo used in the present study has amino acid changes in the S as well as in ORF1a and 1b as compared with the non-virulent Fr-1 strain. Although analysis using recombinant viruses has not yet been done, our result is in good agreement with the observation by Roberts *et al.* in terms of the involvement of the multi-genes in the pathogenicity of SARS-CoV.

The present study suggests involvement of elastase in the development of severe pneumonia caused by SARS-CoV infection. As has been elucidated in cultured cells by Matsuyama *et al.* (17), elastase could enhance SARS-CoV replication in the lung. Alternatively, elastase could be involved in the development of severe respiratory disease via its pathophysiological functions, such as proteolytic activity, enhancement of blood vessel permeability and induction of proinflammatory cytokine secretion (22). These activities of elastase produced in the lungs are reported to be responsible for acute lung injury (22). However, elastase alone is not responsible for the severe respiratory disease described in the present study, since mice infected with *Pp* alone did not develop severe respiratory disease, although it induced as much elastase production as did *Pp* + Fr-mo infection. Thus, extensive infection of SARS-CoV in the lungs could contribute to the development of severe respiratory disease. Studies using elastase inhibitors and anti-elastase antibodies are now in progress to see whether elastase is involved in the pathogenesis of SARS.

There are at least two mechanisms proposed to explain the high pathogenesis of SARS, namely the induction of severe lung injury. Imai *et al.* (34) described that ACE2, the SARS-CoV receptor, plays an important role in preventing

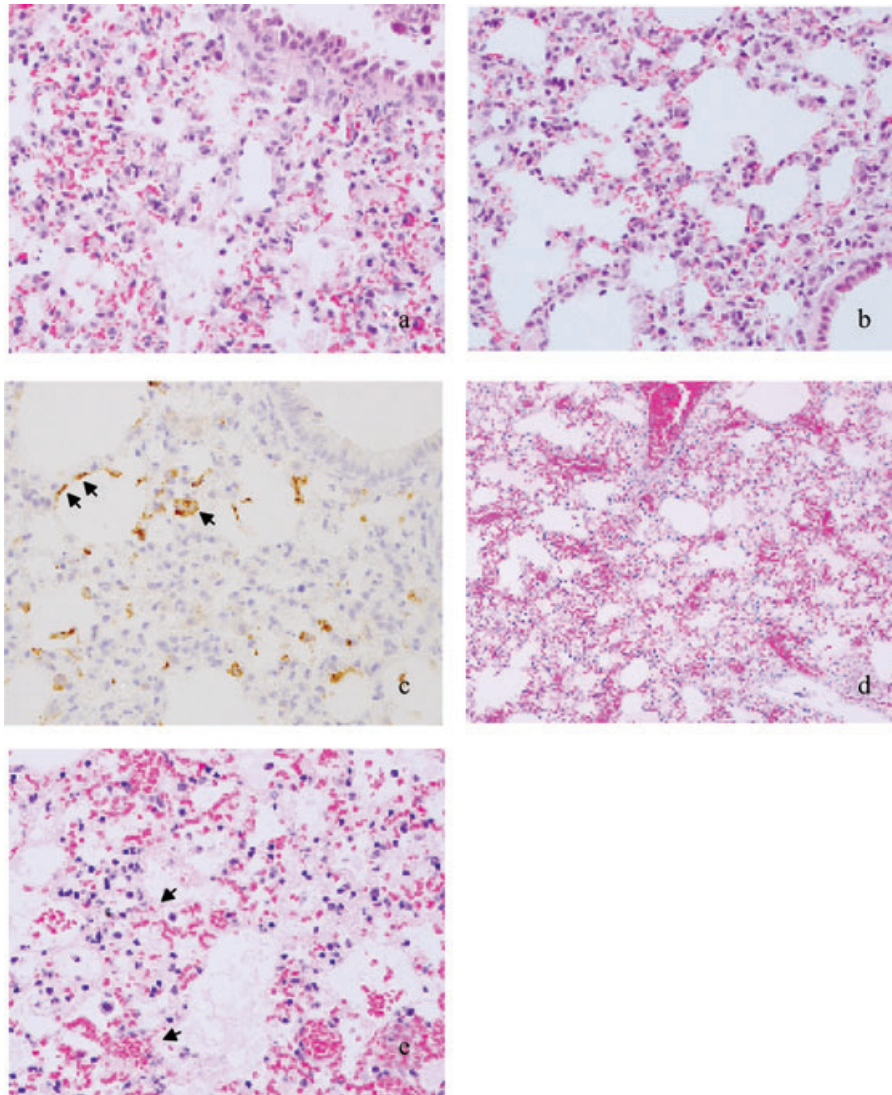


Fig. 6. Histopathological and immunohistochemical studies of lungs infected with *Pp* and/or SARS-CoV. Exudation of hyaline substances into alveolar cavities, infiltration of macrophages and lymphocytes in alveolar walls, and hyperplastic changes of type 2 respiratory epithelial cells were observed in mice co-infected with *Pp* + Fr-mo on day 4 (a), while the exudates in alveoli was not found in mice infected with Fr-mo alone (b). Also, viral antigens (brown) were seen in the cytoplasm of respiratory epithelial cells (arrow) in mice infected with *Pp* + Fr-mo on day four (c). The

lung lesion in the mouse that died on day four after infection by *Pp* + Fr-mo was similar to that seen in cases of diffuse alveolar damage, and was characterized by an exudative hyaline membrane (arrow) in the alveolar cavities (d,e). Antigens were detected with rabbit hyperimmune serum against SARS-CoV using diaminobenzidine for visualization, hematoxylin as a counterstain (c), and hematoxylin and eosin (the others) for routine stains. Original magnification, $\times 30$ (a,b,c and e), $\times 6$ (d).

lung damage and edema by converting angiotensin II with lung damage activity to a less damaging angiotensin₁₋₇. SARS-CoV replication in the lung is known to down-regulate ACE2, resulting in an increase in angiotensin II and lung injury (35). Another mechanism is the severe lung injury caused by cytokines and chemokines produced as a result of SARS-CoV infection. Several different animal models show that high concentrations of inflamma-

tory cytokines could be responsible for the pathogenesis of SARS (9, 13–15). In the present study our hypothesis that high replication of SARS-CoV, presumably due to the presence of proteases that enhance SARS-CoV infection, is responsible for the pathogenesis of SARS does not contradict the above two proposed mechanisms of SARS pathogenesis, since high replication results in greater down-regulation of ACE2 in the lung and also induces higher

cytokine production, as shown in the present study. We believe that the mechanism underlying higher replication of the virus in the lung could be of primary importance in the induction of SARS.

The mortality rate in SARS victims is reported to be approximately 10%, and aged people suffering from chronic heart or renal diseases or diabetes have been shown to be extremely prone to this infection (38). Such individuals are supposed to be susceptible to a variety of infectious agents that normally fail to affect ordinary, healthy individuals. It is possible that exacerbation of SARS in these people could be attributed to co-infection by non- or low-pathogenic agents, such as mycoplasma, chlamydia and the like, although these agents were not often isolated from the patients' lungs (1, 35). However, this does not imply that these agents did not intensify the effects of SARS, since there is a possibility that they may induce a mild inflammation that triggers SARS-CoV's high replication, while failing to themselves grow in the lungs. This may be inferred from the finding in the present study that *Pp* infection exacerbated SARS-CoV infection, but it did not multiply efficiently in the lungs of mice.

Monkeys are not highly susceptible in general to SARS-CoV, though there are reports that they can develop a SARS-like severe respiratory disease (25, 27, 37). This difference in susceptibility might be attributable, in part at least, to the environmental conditions in which monkeys grow up and are maintained during experiments. This hypothesis could also explain why most small laboratory animals, such as mice and rats, appear to not be susceptible to SARS-CoV infection by itself. Such animals are kept "clean" in the sense that they are purposely not exposed to many microorganisms in a laboratory setting. However, if such animals were first contaminated with microorganisms that are normally not virulent, but grow and initiate a mild inflammation in their respiratory organs, they may become sensitive to SARS-CoV infection.

In summary, we have demonstrated that pneumonia caused by SARS-CoV infection can be exacerbated by a co-infection with a low-pathogenic bacterium. This is an excellent animal model for SARS which is extraordinarily important for the development of vaccines and anti-virus drugs, as well as for SARS pathogenesis studies.

ACKNOWLEDGMENTS

We are grateful for the excellent technical assistance of Miyuki Kawase and many helpful discussions from Yasuko Yokota, Koji Ishii, Hideki Hasegawa and Masato Tashiro. We also thank Tetsuya Hagio and Kazuhito Kawabata of Ono Pharmaceutical (Mishima, Osaka, Japan) for their invaluable suggestions on the elastase experiment. This work was financially supported by a grant from the Min-

istry of Health, Labor and Welfare (H16-Shinkoh-9) and a grant from the Ministry of Education, Culture, Sports, Science and Technology (16017308, 17390138).

REFERENCES

1. Drosten C., Gunther S., Preiser W., Van Der Werf S., Brodt H.R., Becker S., Rabenau H., Panning M., Kolesnikowa L., Fouchier R.A., Berger A., Burguiere A.M., Muller S., Rickerts V., Sturmer M., Vieth S., Klenk H.D., Osterhaus A.D., Schmitz H., Doerr H.W. (2003) Identification of a novel coronavirus in patients with severe acute respiratory syndrome. *N Eng J Med* **348**: 1967–76.
2. Kuiken T., Fouchier R.A., Schutten M., Rimmelzwaan G.F., van Amerongen G., van Riel D., Laman J.D., de Jong T., van Doornum G., Lim W., Ling A.E., Chan P.K., Tam J.S., Zambon M.C., Gopal R., Drosten C., van der Werf S., Escriou N., Manuguerra J.C., Stohr K., Peiris J.S., Osterhaus A.D. (2003) Newly discovered coronavirus as the primary cause of severe acute respiratory syndrome. *Lancet* **362**: 263–70.
3. Peiris J.S., Guan Y., Yuen K.Y. (2005) Severe acute respiratory syndrome. *Nat med* **10**: 588–97.
4. Marra M.A., Jones S.J., Astell C.R., Holt R.A., Brooks-Wilson A., Butterfield Y.S., Khattra J., Asano J.K., Barber S.A., Chan S.Y., Cloutier A., Coughlin S.M., Freeman D., Girn N., Griffith O.L., Leach S.R., Mayo M., McDonald H., Montgomery S.B., Pandoh P.K., Petrescu A.S., Robertson A.G., Schein J.E., Siddiqui A., Smailus D.E., Stott J.M., Yang G.S., Plummer F., Andonov A., Artsob H., Bastien N., Bernard K., Booth T.F., Bowness D., Czub M., Drebot M., Fernando L., Flick R., Garbutt M., Gray M., Grolla A., Jones S., Feldmann H., Meyers A., Kabani A., Li Y., Normand S., Stroher U., Tipples G.A., Tyler S., Vogrig R., Ward D., Watson B., Brunham R.C., Krajden M., Petric M., Skowronski D.M., Upton C., Roper R.L. (2003) The genome sequence of SARS-associated coronavirus. *Science* **300**: 1399–404.
5. Rota P.A., Oberste M.S., Monroe S.S., Nix W.A., Campagnoli R., Icenogle J.P., Penaranda S., Bankamp B., Maher K., Chen M.H., Tong S., Tamin A., Lowe L., Frace M., DeRisi J.L., Chen Q., Wang D., Erdman D.D., Peret T.C., Burns C., Ksiazek T.G., Rollin P.E., Sanchez A., Liffick S., Holloway B., Limor J., McCaustland K., Olsen-Rasmussen M., Fouchier R., Gunther S., Osterhaus A.D., Drosten C., Pallansch M.A., Anderson L.J., Bellini W.J. (2003) Characterization of a novel coronavirus associated with severe acute respiratory syndrome. *Science* **300**: 1394–9.
6. Li W., Moore M.H., Vasileva N., Sui J., Wong S.K., Berne M.A., Somasundaran M., Sullivan J.L., Luzuriaga K., Greenough T.C., Choe H., Farzan M. (2003) Angiotensin-converting enzyme 2 is a functional receptor for the SARS coronavirus. *Nature* **426**: 450–4.
7. Fouchier R.A., Kuiken T., Schutten M., Amerongen G.V., Van Doornum G.J., Van Den Hoogen B.G., Peiris M., Lim W., Stohr K., Osterhaus D. (2003) Aetiology: Koch's postulates fulfilled for SARS virus. *Nature* **423**: 240.
8. Martina B.E., Haagmans B.L., Kuiken T., Fouchier R.A., Rimmelzwaan G.F., Van Amerongen G., Peiris J.S., Lim W., Osterhaus A.D. (2003) SARS virus infection of cats and ferrets. *Nature* **425**: 915.
9. Nagata N., Iwata N., Hasegawa H., Fukushi S., Yokoyama M., Harashima A., Sato Y., Saijo M., Morikawa S., Sata T. (2007) Participation of both host and virus factors in induction of severe acute respiratory syndrome (SARS) in F344 rats infected with SARS coronavirus. *J Virol* **81**: 1848–57.
10. Roberts A., Paddock C., Vogel L., Butler S., Zaki S., Subbarao K. (2005) Aged BALB/c mice as a model for increased severity of severe acute respiratory syndrome in elderly humans. *J Virol* **79**: 5833–8.

11. Subbarao K., McAuliffe J., Vogel L., Fahle G., Fischer S., Tatti K., Packard M., Shieh W.J., Zaki S., Murphy B. (2004) Prior infection and passive transfer of neutralizing antibody prevent replication of severe acute respiratory syndrome coronavirus in the respiratory tract of mice. *J Virol* **78**: 3572–7.
12. Weiss S.R., Navas-Martin S. (2005) Coronavirus pathogenesis and the emerging pathogen severe acute respiratory syndrome coronavirus. *Microbiol. Mol Biol Rev* **69**: 635–64.
13. McCray P.B. Jr, Pewe L., Wohlford-Lenane C., Hickey M., Manzel L., Shi L., Netland J., Jia H.P., Halabi C., Sigmund C.D., Meyerholz D.K., Kirby P., Look D.C., Perlman S. (2007) Lethal infection of K18-hACE2 mice infected with severe acute respiratory syndrome coronavirus. *J Virol* **81**: 813–21.
14. Tseng C.T., Huang C., Newman P., Wang N., Narayanan K., Watts D.M., Makino S., Packard M., Zaki S.R., Chan T.S., Peters C.J. (2007) SARS coronavirus infection of mice transgenic for the human angiotensin-converting enzyme 2 (hACE2) virus receptor. *J Virol* **81**: 1162–73.
15. Roberts A., Deming D., Paddock C., Cheng A., Yount B., Vogel L., Herman B., Sheahan T., Heise M., Genrich G., Zaki S., Baric R., Subbarao K. (2007) A Mouse-adapted SARS-coronavirus causes disease and mortality in BALB/c mice. *PLoS Pathogens* **3**: 23–37.
16. Poutanen S.M., Low D.E., Henry B., Finkelstein S., Rose D., Green K., Tellier R., Draker R., Adachi D., Ayers M., Chan A.K., Skowronski D.M., Salit I., Simor A.E., Slutsky A.S., Doyle P.W., Krajden M., Petric M., Brunham R.C., McGeer A.J. (2003) Identification of severe acute respiratory syndrome in Canada. *N Engl J Med* **348**: 1995–2005.
17. Matsuyama S., Ujike M., Morikawa S., Tashiro M., Taguchi F. (2005) Protease-mediated enhancement of severe acute respiratory syndrome coronavirus infection. *Proc Natl Acad Sci USA* **102**: 12543–7.
18. Thiel V., Ivanov K.A., Putics A., Hertzog T., Schelle B., Bayer S., Weissbrich B., Snijder E.J., Rabenau H., Doerr H.W., Gorbalenya A.E., Ziebuhr J. (2003) Mechanisms and enzymes involved in SARS coronavirus genome expression. *J Gen Virol* **84**: 2305–15.
19. Nakagawa M., Saito M. (1984) Antigenic characterization of *Pasteurella pneumotropica* isolated from mice and rats. *Jikken Dobutsu* **30**: 313–6.
20. Yoshimura K., Nakagawa S., Koyama S., Kobayashi T., Homma T. (1994) Roles of neutrophil elastase and superoxide anion in leukotriene B₄-induced lung injury in rabbit. *J Appl Physiol* **76**: 91–6.
21. Jacoby R.O., Fox J.G., Davisson M. (2002) In: *Laboratory Animal Medicine*. New York: Academic Press, pp. 35–120.
22. Kawabata K., Hagio T., Matsuoka S. (2002) The role of neutrophil elastase in acute lung injury. *Eur J Pharmacol* **451**: 1–10.
23. Nicholls J.M., Poon L.L.M., Lee K.C., Ng W.F., Lai S.T., Leung C.Y., et al (2003) Lung pathology of fatal severe acute respiratory syndrome. *Lancet* **361**: 1773–8.
24. Tse G.M.K., To K.F., Chan P.K.S., Lo A.W.I., Ng K.C., Wu A., et al (2004) Pulmonary pathological features in coronavirus associated acute respiratory syndrome (SARS). *J. Clin. Pathol.* **57**: 260–5.
25. Glass W.G., Subbarao K., Murphy B., Murphy P.M. (2004) Mechanism of host defense following severe acute respiratory syndrome-coronavirus (SARS-CoV) pulmonary infection of mice. *J Immunol* **173**: 4030–9.
26. Roberts A.L., Guarner V.J., Hayes N., Murphy B., Zaki S., Subbarao K. (2005) Severe acute respiratory syndrome coronavirus infection of golden Syrian hamsters. *J Virol* **79**: 503–11.
27. Greenough T.C., Carville C.A., Coderre J., Somasundaran M., Sullivan J.L., Luzuriaga K., Manfield K. (2005) Pneumonia and multi-organ system disease in common marmosets (*Callithrix jacchus*) infected with severe acute respiratory syndrome-associated coronavirus. *Am J Pathol* **167**: 455–63.
28. Qin C., Wang J., Wei Q., She M., Marasco W.A., Jiang H., Tu X., Zhu H., Ren L., Gao H., Guo J., Huang L., Yang R., Cong Z., Wang Y., Liu Y., Sun L., Duan S., Qu J., Chen L., Tong W., Ruan L., Liu P., Zhang H., Zhang J., Liu D., Liu Q., Hong T., He W. (2005) An animal model of SARS produced by infection of Macaca mulatta with SARS coronavirus. *J Pathol* **206**: 251–9.
29. Weingartl H., Czub M., Czub S., Neufeld J., Marzal P., Gren J., Smith G., Jones S., Proulx R., Deschambault Y., Brudeski E., Andonov A., He R., Li Y., Copps J., Grolla A., Dick D., Berry J., Ganske S., Manning L., Cao J. (2004) Immunization with modified vaccinia virus Ankara-based recombinant vaccine against severe acute respiratory syndrome is associated with enhanced hepatitis in ferrets. *J Virol* **78**: 12672–6.
30. Li W., Zhang C., Sui J., Kuhn J.H., Moore M.J., Luo S., Wong S.K., Huang I.C., Xu K., Vasillieva N., Murakami A., He Y., Marasco W.A., Guan Y., Choe H., Farzan M. (2005) Receptor and viral determinants of SARS-coronavirus adaptation to human ACE2. *EMBO J* **24**: 1634–43.
31. The Chinese S.A.R.S. Molecular E.pidemiology Consortium. (2004) Molecular evolution of the SARS coronavirus during the course of the SARS epidemic in China. *Science* **303**: 1666–9.
32. Iacono K.T., Kazi L., Weiss S.R. (2006) Both spike and background genes contribute to murine coronavirus neurovirulence. *J Virol* **80**: 6834–43.
33. Phillips J.J., Chua M.M., Lavi E., Weiss S.R. (1999) Pathogenesis of chimeric MHV4/MHV-A59 recombinant viruses: the murine coronavirus spike protein is a major determinant of neurovirulence. *J Virol* **73**: 7752–60.
34. Imai Y., Kuba K., Rao S., Huan Y., Guo F., Guan B., Yang P., Sarao R., Wada T., Leong-poi H., Crackower H.A., Fukamizu A., Hui C., Hein L., Uhling S., Slutsky A.S., Jiang C., Penninger J.M. (2005) Angiotensin-converting enzyme 2 protects from severe acute lung failure. *Nature* **436**: 112–6.
35. Kuba K., Imai Y., Rao S., Gao H., Guo F., Guan B., Huan Y., Yang P., Zhang Y., Deng W., Bao L., Zhang B., Liu G., Wang Z., Chappell M., Liu Y., Zheng D., Leibbrandt A., Wada T., Slutsky A.S., Liu D., Qin C., Jiang C., Penninger C.M. (2005) A crucial role of angiotensin converting enzyme 2 (ACE 2) in SARS coronavirus-induced lung injury. *Nat Med* **11**: 875–9.
36. Ksiazek T.G., Erdman D., Goldsmith C.S., Zaki S.R., Peret T., Emery S., Tong S., Urbani C., Comer J.A., Lim W., Rollin P.E., Dowell S.F., Ling A.E., Humphrey C.D., Shieh W.J., Guarner J., Paddock C.D., Rota P., Fields B., DeRisi J., Yang J.Y., Cox N., Hughes J.M., LeDuc J.W., Bellini W.J., Anderson L.J. (2003) A novel coronavirus associated with Severe acute respiratory syndrome. *N Engl J Med* **348**: 1953–66.
37. Rowe T., Gao G., Hogan R.J., Crystal R.G., Voss T.G., Grant R.L., Bell P., Kobinger G.P., Wivel N.A., Wilson J.M. (2004) Macaque model for severe acute respiratory syndrome. *J Virol* **78**: 11401–4.
38. Peiris J.S., Yuen K.Y., Osterhaus A.D., Stohr K. (2003) The severe acute respiratory syndrome. *New Engl. J. Med.* **349**: 2431–41.